β-Sheet Containment by Flanking Prolines: Molecular Dynamic Simulations of the Inhibition of β-Sheet Elongation by Proline Residues in Human Prion Protein

Mohd S. Shamsir* and Andrew R. Dalby†

*Biology Department, Faculty of Science, Universiti Teknologi Malaysia, 81310 Skudai, Johor; and †Department of Statistics, School of Statistics, University of Oxford, Oxford OX1 3SY, United Kingdom

ABSTRACT Previous molecular dynamic simulations have reported elongation of the existing β-sheet in prion proteins. Detailed examination has shown that these elongations do not extend beyond the proline residues flanking these β-sheets. In addition, proline has also been suggested to possess a possible structural role in preserving protein interaction sites by preventing invasion of neighboring secondary structures. In this work, we have studied the possible structural role of the flanking proline residues by simulating mutant structures with alternate substitution of the proline residues with valine. Simulations showed a directional inhibition of elongation, with the elongation progressing in the direction of valine including evident inhibition of elongation by existing proline residues. This suggests that the flanking proline residues in prion proteins may have a containment role and would confine the β-sheet within a specific length.

INTRODUCTION

Prions are a transmissible agent consisting of an abnormal isoform of the prion protein (PrP), designated PrPSC (1). PrPSC (SC for scrapie) is derived from a posttranslational conformational transformation (2,3) of the cellular isoform, PrPC (C for cellular) (4,5). The term ''prion'' is a dyslexic acronym (6) coined by Prusiner for ''proteinaceous infectious particle'' to define a small proteinaceous infectious particle that resists inactivation by procedures which modify nucleic acids (7). According to the ''protein only'' hypothesis, prion propagation involves a novel concept of transmission by proteinaceous material alone, which is able to convert other normal isoforms to itself in an autocatalytic manner causing infection and disease proliferation without the transmission of a nucleic acid genome. PrP is unique in that it goes against two main dogmas in molecular biology. First, PrP has shown that pathogens are able to replicate in the absence of nucleic acids. Second, PrP defies the ''one sequence, one conformation'' dogma because the conformation of the normal PrP sequence can transform into a different pathogenic conformation, either spontaneously or by association with repreexisting pathogenic material (8). Prion diseases or transmissible spongiform encephalopathies are characterized by spongiform degeneration and the accumulation of PrPSC in the brain. Prion diseases can also be grouped under the more general term of conformational diseases such as α1-antitrypsin deficiency, sickle cell anemia, and familial amyloid polyneuropathy as all these diseases have comparable inherent conformational instability of a specific protein that results in its deposition in the tissue of the affected organism (9,10).

There are 15 proline residues in the human PrP structure, with 12 residues in the flexible N-terminus. The 12 proline residues in the N-terminus are periodic and conformationally stabilized by copper (11). The other three proline residues are located within the globular domain of PrPC. The antiparallel β-sheet consisting of strand S2 is flanked at both ends by Pro-158 and Pro-165, with the opposing strand S1 flanked by a single proline at position 137 (Fig. 1). Proline is an amino acid that has a pyrrolidine ring structure that prevents participation in the usual hydrogen bonding between NH and CO groups of other amino acids. The presence of the ring causes proline to be disfavored in β-sheet structure as its ϕ-angle is incompatible and it lacks one potential H-bond donor (12). Consequently, this makes its occurrence in β-sheet rare. In fact, the rare occurrences of proline in secondary structure have led to the practice of systematically substituting proline in mutagenesis studies, thus becoming a practical tool to identify segments involved in protein aggregation (13). Proline residues are more frequently found in sharp turns linking β-strands (β-bends), kinks in transmembrane α-helices, at the edges of β-sheets or, most frequently, within loops and disordered regions of proteins (13).

Previously, we have performed MD simulations at denaturing temperatures, and residual structures have shown evidence that suggested that the elongation of S1 and S2 in the PrP is restricted and did not proceed beyond Pro-158 and Pro-165 flanking both sides of S2 and beyond Pro-137 on the C-terminal end of S1 (14). Other MD simulations have also shown similar restrictions (15–18) even at elevated temperatures (19). The zipper-like progression of sheet formation could therefore be prevented by the presence of these proline ''brackets''.

A study has also shown that proline is the residue most commonly found in the flanking segments of protein-protein

Submitted June 27, 2006, and accepted for publication November 16, 2006.

Address reprint requests to Andrew R. Dalby, E-mail: dalby@stats.ox.ac.uk.

0006-3495/07/03/2080/10 $2.00

doi: 10.1529/biophysj.106.092320

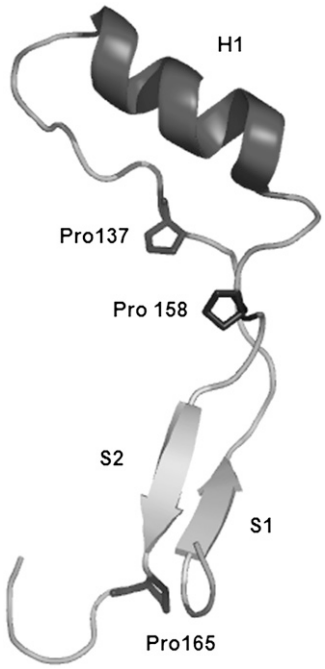

FIGURE 1 Ribbon diagram of S1 (sheet 1), S2 (sheet 2), and H1 (helix 1), with proline indicated by its ring. The diagram shows only S1, S2, and H1, with H2 (helix 2) and H3 (helix 3) omitted for clarity. The secondary structures are presented with helices and sheets.

interaction sites (20). Examination of over 1600 protein-protein interaction sites indicated that proline residues are commonly found within these flanking segments and the probability of occurrence in flanking segments is 2.5 times greater than elsewhere in the structure (20). As a result, proline brackets have been proposed to perform a structural role in protecting the conformation and integrity of the interaction site by blocking the ''invasion'' of neighboring secondary structures (20). Investigation of the properties of proline-delimited regions has also led to the discovery of the L-type Ca^{2+} channel binding site of calciseptine (21).

TABLE 2 Variants of proline/valine construct used in the MD simulations

Variant	1QLX	PPV	PVV	PVP	VPP	VVP	VPV	VVV
Res 135	P	P	P	P	V	V	V	V
Res 158	P	P	V	V	P	V	P	V
Res 165	P	V	V	P	P	P	V	V

The presence of proline residues at the edge of the β-sheet has also been proposed as a negative design feature to avoid aggregation and essentially to serve as a capping mechanism (22). A survey of all the prion structures available in the Protein Data Bank (PDB) revealed that proline bracket is present and that the secondary structure architecture of the S2 strand is highly conserved in the different species, as expected from the high degree of sequence identity (Table 1).

This work follows our earlier observations regarding the expansion of β-sheet (14) and examines if the existence of proline residues flanking β-strands' S1 and S2 has a role in restraining the zippering process of the β-strands, therefore maintaining its length to a fixed number of residues. Variants with alternating proline substitutions have been used to examine if specific proline residues play a distinct role in restraining the β-sheet.

MATERIALS AND METHODS

The starting structure for all the simulations was based on the NMR structure of the human PrP domain designated in PDB as 1QLX (23), which contains the C-terminal globular structure of human prion consisting of residues 125–228. The structure 1QLX was used as wild-type, and the variant structures were constructed using Deep View (24) by alternate substitution of proline with valine at position 135, 158, and 165 (Fig. 1), creating seven mutant variants which were used for the simulations (Table 2).

The remainder of the structure is left unaltered. The disulphide bond between H2 and H3 was left intact as previous work showed that it remains oxidized in PrPSC and necessary for infectivity (25,26). All models were solvated in a box of explicit simple point charge water molecules and simulated using periodic boundary conditions and particle mesh Ewald summation that have been shown to improve electrostatic interactions (27). Structures were

TABLE 1 Amino acid sequence alignment of the fragment 158–173 for the different species

PDB ID	Species	157	158	159	160	161	162	163	164	165	166	167	168	169	170	171	172	173
1QLX	Human	Y	P	N	Q	**V**	**Y**	**Y**	R	P	M	D	E	Y	S	N	Q	N
1AG2	Mouse	Y	P	N	Q	**V**	**Y**	**Y**	R	P	V	D	Q	Y	S	N	Q	N
1B10	Hamster	Y	P	N	Q	**V**	**Y**	**Y**	R	P	V	D	Q	Y	N	N	Q	N
1DWY	Bovine	Y	P	N	Q	**V**	**Y**	**Y**	R	P	V	D	Q	Y	S	N	Q	N
1UW3	Sheep	Y	P	N	Q	**V**	**Y**	**Y**	R	P	V	D	R	Y	S	N	Q	N
1XYJ	Cat	Y	P	N	Q	**V**	**Y**	**Y**	R	P	V	D	Q	Y	S	N	Q	N
1XYQ	Pig	Y	P	N	Q	**V**	**Y**	**Y**	R	P	V	D	Q	Y	S	N	Q	N
1XYW	Elk	Y	P	N	Q	**V**	**Y**	**Y**	R	P	V	D	Q	Y	N	N	Q	N
1XYK	Dog	Y	P	N	Q	**V**	**Y**	**Y**	R	P	V	D	Q	Y	N	N	Q	S
1XU0	Frog	M	P	N	R	**V**	–	**Y**	R	P	M	Y	R	G	E	E	Y	V
1U3M	Chicken	Y	P	N	R	**V**	**Y**	**Y**	R	D	Y	S	S	–	–	P	V	P
1U5L	Turtle	Y	P	N	R	**V**	**Y**	**Y**	K	E	Y	N	D	R	–	S	V	P

The table shows NMR determined structures deposited in the PDB. It uses human sequence numbering with flanking proline residues underlined and β-sheet assigned structure consisting of amino acid residues. VYY is highlighted in bold.

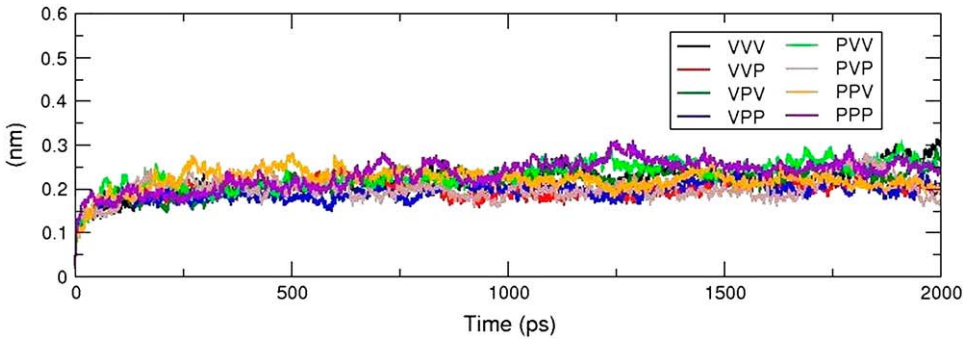

FIGURE 2 RMSDs of all proline variants as a function of time for all proline variants.

minimized using 200 steps of the steepest descent method. Simulations were performed using the GROMACS 3.1.4 package and the all-hydrogen function GROMOS96 (28). Simulations were carried out at 300 K and 500 K, and isotropic pressure coupling was applied. All systems were equilibrated for 200 ps of solute position restrained molecular dynamics (MD). Unrestrained MD was performed on all variants for 2 ns with a LINCS algorithm 2-fs time step for each system. Simulations that showed a significant increase in β-sheet structure were repeated over a longer 10-ns timescale. Simulations were performed at pH 7. All the resulting trajectories were analyzed using GROMACS utilities. The C_α root mean-square deviations (RMSDs) and C_α root mean-square fluctuations (RMSFs) relative to the average MD structure were calculated. The DSSP program was used to determine the percentage of secondary structure throughout the simulations (29). Protein structure images were created using PyMOL (30) and Protein Explorer (31).

RESULTS AND DISCUSSION

Structural deviations and fluctuations

Fig. 2 shows the RMSD from the NMR structure as a function of simulation time for the C_α atom in each variant. Fig. 3 shows that the RMSF from the NMR structure is a function of residue number for the C_α atom in each variant. The MD simulation showed that all variants were stable throughout the simulation. The C_α RMSD values for all eight variants increased during the first 0.1 ns before reaching a plateau at 0.15−0.3 ns (Fig. 2). The RMSFs of all variants showed that highest fluctuations occurred in the N-terminus and the loop between helices (H2 and H3) (Fig. 3), whereas the globular domain containing H2 and H3 remains relatively stable. Consequently, this created the groove pattern observed in reported MD simulations (14,17,19,32,33). The absence of rigid constraints imposed by proline residues on the N-C_α rotation in mutated structures did not substantially increase the fluctuations of the global conformation.

β-sheet content

Fig. 4, *a–h*, shows the number of residues forming β-sheets as a function of simulation time determined with DSSP. Only two variants, VVV (Fig. 4 *a*) and PVV (Fig. 4 *c*), exhibited an increase in the number of residues participating in the β-sheet formation. MD simulation of VVV showed a discernible pair-like addition of two residues at a time at 0.5 ns and 1.6 ns (Fig. 4 *a*), suggesting a zippering process (34). A two-residue extension occurred with the addition of four participating residues at the end of the simulation. MD simulation of PVV showed a similar but faster pair-like increase during the first 0.2 ns. However, the extension in PVV exhibited higher fluctuations than VVV. The rest of the variants did not show a sustained increase in residue number and only showed fluctuations at around six residues (Fig. 4, *b* and *d–h*). The wild-type structure PPP showed the biggest fluctuations in β-sheet content ranging between 0 and 7 residues (Fig. 4 *g*).

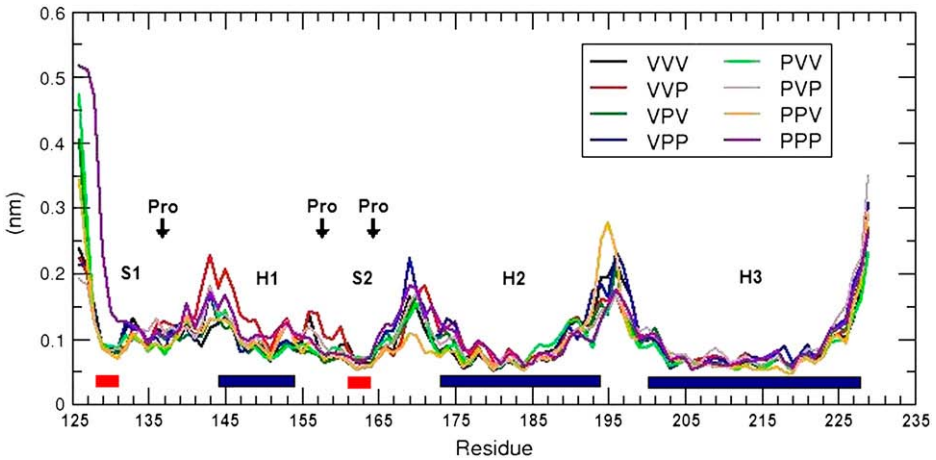

FIGURE 3 RMSFs of all proline variants with residues numbered according to the human prion residue sequence; blue bars denote α-helices, red bars β-sheets in wild-type structure; S1, sheet 1; S2, sheet 2; H1, helix 1; H2, helix 2; H3, helix 3, and black arrows indicate the position of proline residues in the protein sequence.

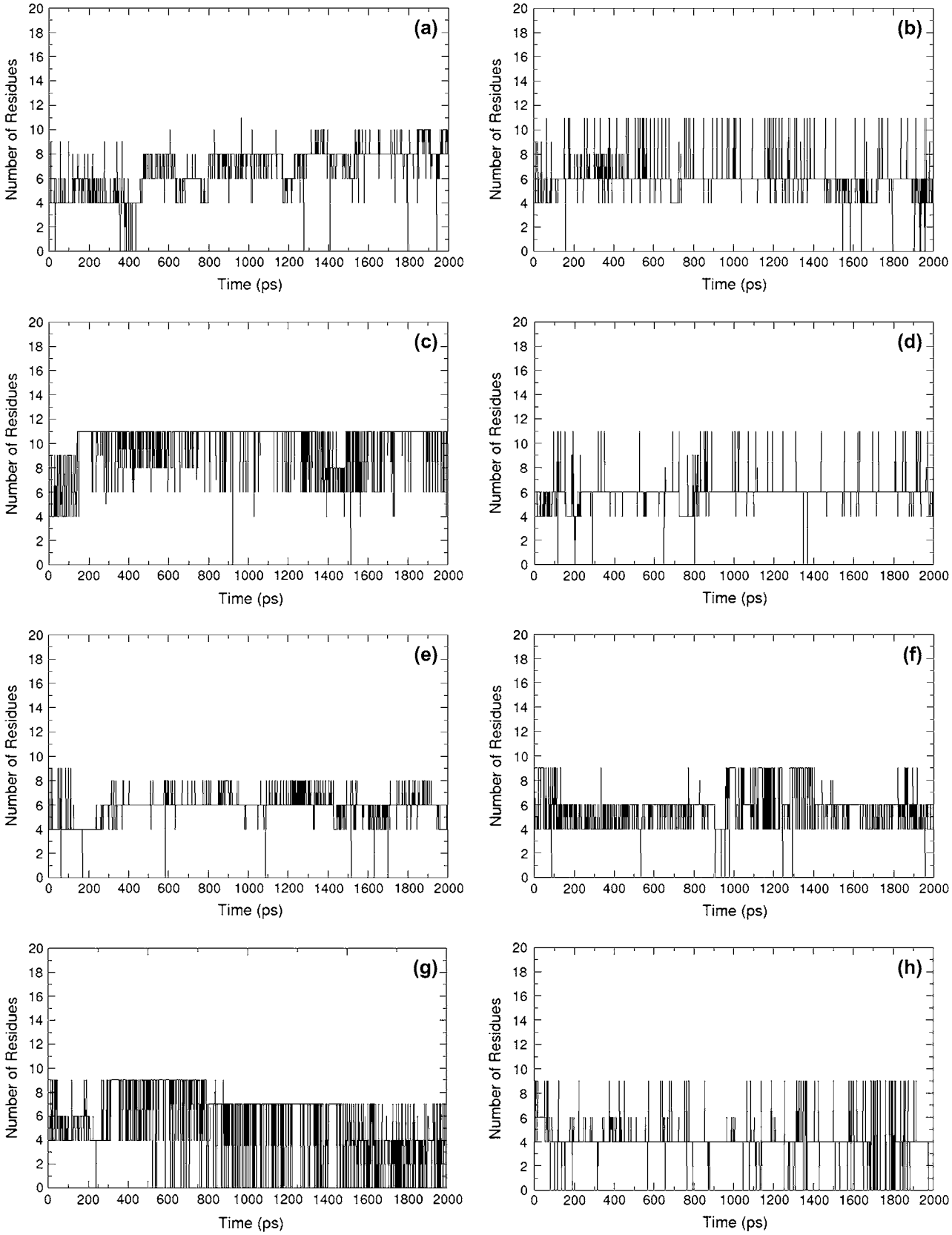

FIGURE 4 Number of residues forming β-sheets as a function of simulation time determined with DSSP during the simulation (*a*) VVV, (*b*) VPV, (*c*) PVV, (*d*) PPV, (*e*) PVP, (*f*) VVP, (*g*) PPP, and (*h*) VPP.

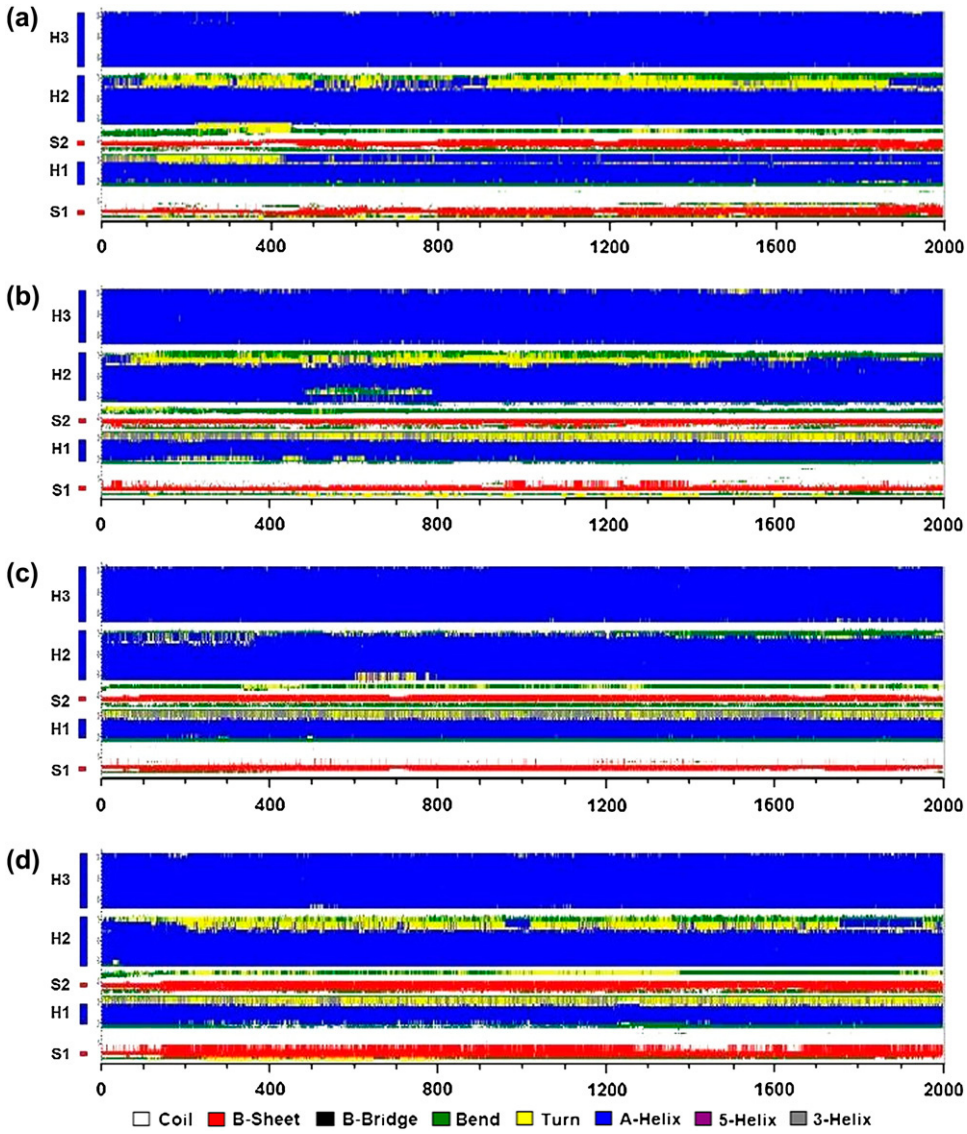

FIGURE 5 Secondary structure of variants as a function of simulation time determined by DSSP. The diagram shows (*a*) VVV, (*b*) VVP, (*c*) VPV, and (*d*) PVV variants. H1, H2, and H3 denote helices 1, 2, and 3. S1 and S2 denote sheet 1 and sheet 2. The color guide denotes types of secondary structure.

Structural evolutions: elongation of existing β-sheets

Figs. 5, *a–d*, and 6, *a–d*, show the evolution of the secondary structures during the MD simulation as determined by DSSP. In all the simulations, the increase of β-sheets occurred through the extension of existing secondary structure and not by creation of new β-structures anywhere else in the protein structure.

Analysis of the secondary structure evolution revealed several interesting observations. The presence of the Pro-158 and Pro-165 flanking S2 seems to hinder the elongation of β-sheet S1 and S2, and its removal seems to induce β-sheet elongation. In VVV and PVV where these two proline residues have been replaced, the elongation occurred in both directions. In other variants, the expansion occurs away from an existing proline residue, thus creating a directional pattern (Fig. 7). The presence of Pro-137 residue did not prevent sheet elongation. This is probably because Pro-137 is three residues farther down the sequence and elongation may therefore occur on a longer timescale. Previous MD simulations have reported elongation of S1 and S2 (15,16,18,35–37) where all elongation of S2 was limited to within the six residues between Pro-158 and Pro-165.

Mechanism of elongation

The MD simulation trajectories for VVV, PVV, and PPP were examined by superimposing sequential coordinate snapshots of structures to examine its conformational changes. The trajectory of VVV showed low fluctuations about the secondary structure and did not exhibit any major departure from the NMR structure. The reduced mobility of the residues Leu-125-Gly-126-Gly-127-Tyr-128 of the N-terminus is evident by its movement into the globular structure as the

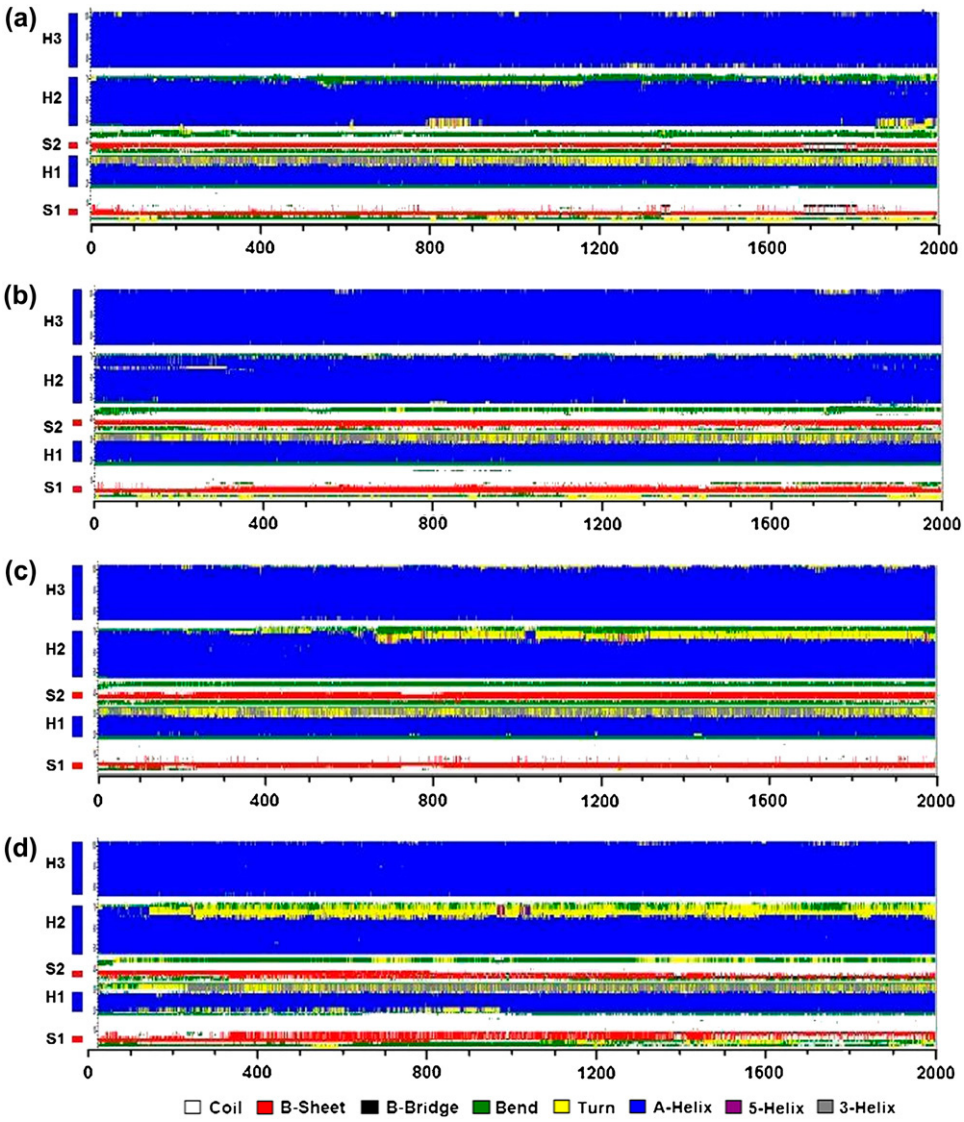

FIGURE 6 Secondary structure of variants as a function of simulation time determined with DSSP. The diagram shows (*a*) VPP, (*b*) PVP, (*c*) PPV, and (*d*) PPP variants. H1, H2, and H3 denote helices 1, 2, and 3. S1 and S2 denote sheet 1 and sheet 2. The color guide denotes types of secondary structure.

zippering process realigns it to elongate the β-sheet. The fluctuations are constrained by the alignment process of the N-terminus, which results in the low RMSF range of 0.1–0.25 nm. In contrast, the Leu-125-Gly-127-Gly-127-Tyr-128 residues of PPP exhibited higher mobility due to the absence of the zippering and realignment process in VVV, as exemplified by the higher RMSF range of 0.1−0.5 nm. The trajectory of PVV exhibits intermediate behavior with partial zippering and alignment. The Leu-125-Gly-126-Gly-127-Tyr-128 residues also showed reduced fluctuations compared to PPP. In contrast to the N-terminus, residues forming segments between S1 and S2 that include H1 showed higher mobility in VVV compared to PPP and PVV. These increased fluctuations could be attributed to the absence of rigidity that Pro-137 residues imposed on the N-C_α rotation, consequently limiting the plasticity of the same segment in PVV and PPP. The global stability of the structure and realignment of the N-terminus suggest that the elongation of β-sheet occurs through the ability of valine to form hydrogen bonding after substituting proline, thus allowing the zippering process to continue.

Extended simulations

Extended MD simulations were performed to examine structural stability over a longer simulation period. Three variants—VVV, PVV, and PPP—and chicken prion 1U3M were simulated. VVV and PVV were selected, as both showed an extended zippering of the β-sheet compared to the other variants, and PPP is selected as a control representing the wild-type structure. 1U3M was chosen as the chicken prion structure (38) has a different proline trimer sequence at position 151-165-176, with ~30% sequence identity, and is expected to show different conformational behavior.

Fig. 8, *a–d*, shows the evolution of the secondary structures and Fig. 9, *a–d*, shows the β-sheets' content of each

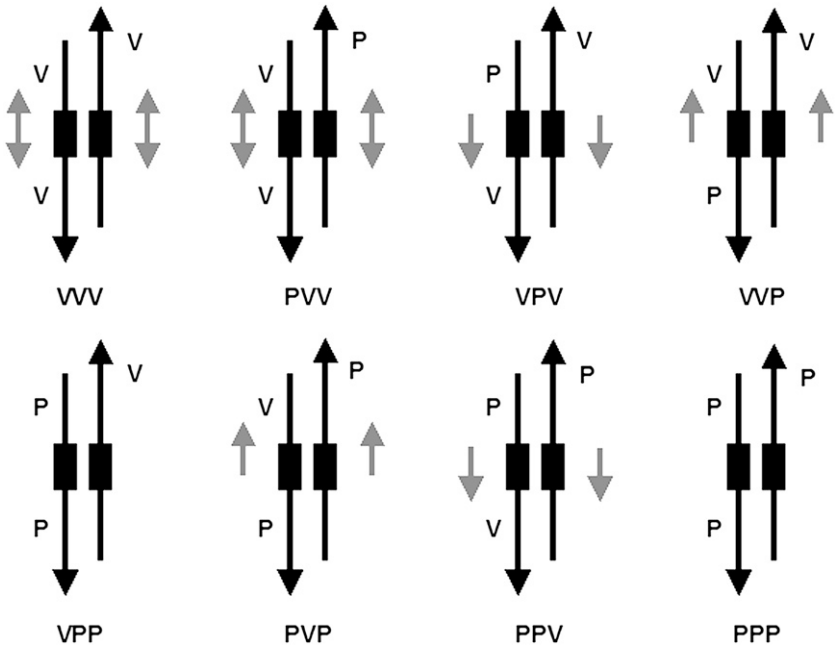

FIGURE 7 Schematic diagram of the direction of the β-sheet expansion. The diagram shows the schematic of β-sheet expansion of all proline variants. The antiparallel β-sheets are denoted by a pair of black boxes, the direction of the polypeptide is denoted by the black arrow, and the presence and direction of expansion are in gray arrows.

variant as determined by DSSP for (*a*) PVV, (*b*) PPP, (*c*) 1U5L, and (*d*) VVV, respectively. The result for PVV, PPP, and VVV is similar to their initial runs where the increase of β-sheets occurred through the extension of the existing secondary structure and not by creation of new β-structures anywhere else in the protein structure. The simulation is also stable without any changes in the overall protein conformation. The C_α RMSD values for all three variants stabilized after 0.3 ns and the C_α RMSF of all variants showed a similar groove pattern signature observed in the 2-ns MD simulation and to other reported MD simulations (14,17,19,32,33). The PVV variant showed a 100% increase in the number of residues participating in the β-sheet elongation to 13 residues similar to the initial 2-ns MD simulation (Fig. 9 *a*). The longer simulation showed the β-sheet formation stabilizing at 4.4 ns and showed similar elongation mechanism to the earlier MD. The VVV variant also showed similar behavior to the initial MD but with a higher degree of structural fluctuation in residues forming segments between S1 and S2 that include H1 compared to PVV. These larger fluctuations are exemplified by the failure to recruit adjacent residues to extend the β-sheet, thus limiting the residue participation to eight amino acids (Fig. 9 *d*). In addition, the PPP variant also behaved in a similar manner to the initial MD simulation with the number of participating residues limited to between six and nine (Fig. 9 *b*). The chicken prion also showed similar global conformational behavior with the other three variants (Fig. 8 *c*). The secondary structures were maintained throughout the MD simulation but with larger fluctuations. The β-sheet content fluctuated throughout the simulation, with the number of residues forming β-sheets fluctuating between 8 and 10 residues, similar to the ranges shown by VVV (Fig. 9 *c*). There was a temporary increase in the number of residues participating in β-sheet formation between 1 ns and 2 ns via the formation of a turn at the N-terminal and the creation of unstable triple-stranded β-sheets (Fig. 8 *c*).

CONCLUSIONS

MD simulation of proline-substituted structures showed that removal of proline residues induces directional elongation of the β-sheet. The extended 10-ns MD simulations have also shown that the β-sheet structure is stable for certain variant (PVV) but not VVV. This suggests that substituting all of the proline residues would reduce structural rigidity and increase fluctuations, therefore decreasing the propensity for adjacent strands to align and form β-sheets. It also showed that the wild-type variant (PPP) did not increase the β-sheet content at the end of the simulation. Simulation of the chicken prion did not show an increase even though the proline brackets were farther apart than the human prion, suggesting other factors might contribute to the failure of the β-sheet to expand. This is not surprising as the low sequence identity with human PrP might provide altered dynamics compared to mammalian-derived PrPs. Further work needs to be done to study the MD signature of chicken as well as other nonmammalian prions such as those of turtles and frogs (38).

The elongation occurred via a zippering process that is discernible by a pairing pattern caused by sequential recruitment of residues in pairs. Therefore, when the zipper-like process is halted by the flanking proline in the structure, this suggests that proline residues act as a steric barrier by restricting the number of residues to six within the proline bracket of Pro-158 and Pro-165. Interestingly, the six-residue

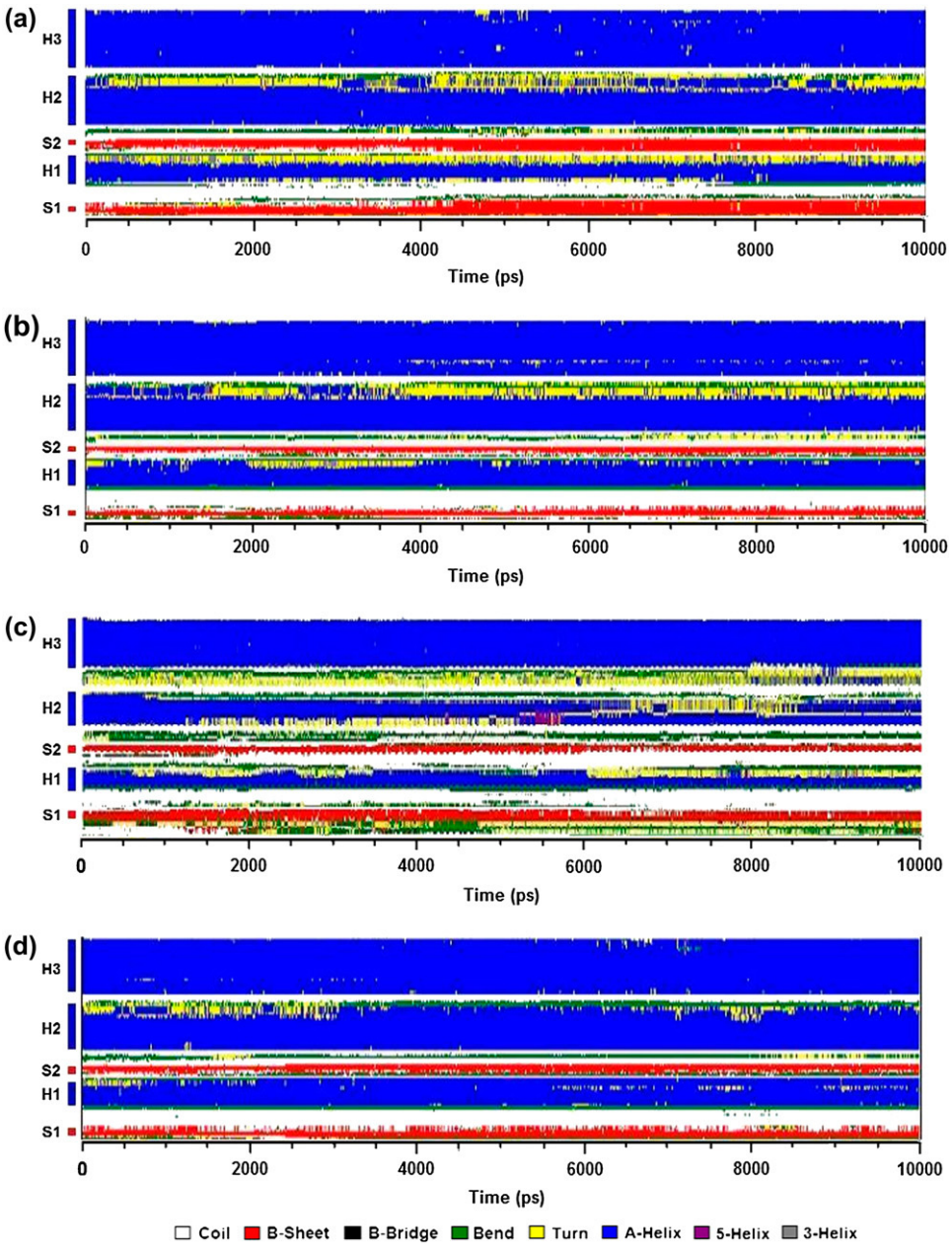

FIGURE 8 Secondary structure as a function of simulation time determined with DSSP during the simulation: (*a*) PVV, (*b*) PPP, (*c*) 1U3M, and (*d*) VVV; S1, sheet 1; S2, sheet 2; H1, helix 1; H2, helix 2; H3, helix 3. The color guide designates types of secondary structure.

length is near the intrinsic limit of conformational stability in antiparallel β-sheet. Studies have shown that at least for some antiparallel sequences, the conformational stability increases with strand length to a maximum of seven residues (39). The proline bracket has also been shown to confine the secondary structures within its boundary even in elevated temperature. In contrast, the lone proline at residue 137 does not play a role in this bracket but seems to contribute only to the structural rigidity of the segment between S1 and S2. If the presence of the proline brackets is instrumental in determining and maintaining the length of the β-sheet to a fixed number of residues, there is a possibility that the length of additional β-sheet propagated by the residues 90–124 of the flexible N-terminus (17) must not exceed a certain length of the seed strand (S2). Models of possible prion protofibrils created using electron crystallography data showed preservation of β-sheet length within the proline bracket, thus reinforcing its possible role in determining β-sheet length (40,41). Analysis of sequence evolutionary conservation in 27 mammalian and 9 avian PrPC has shown that the proline bracket segment PNQVYYRP is highly conserved (42). In addition, the segment XPNXVY that contains Pro-158 has a higher than average sequence conservation and appears to be needed for the stability of the ''PrP-fold'' (38). Experimentally, studies have shown that the existence of proline residues plays a significant role in protein conformational stability

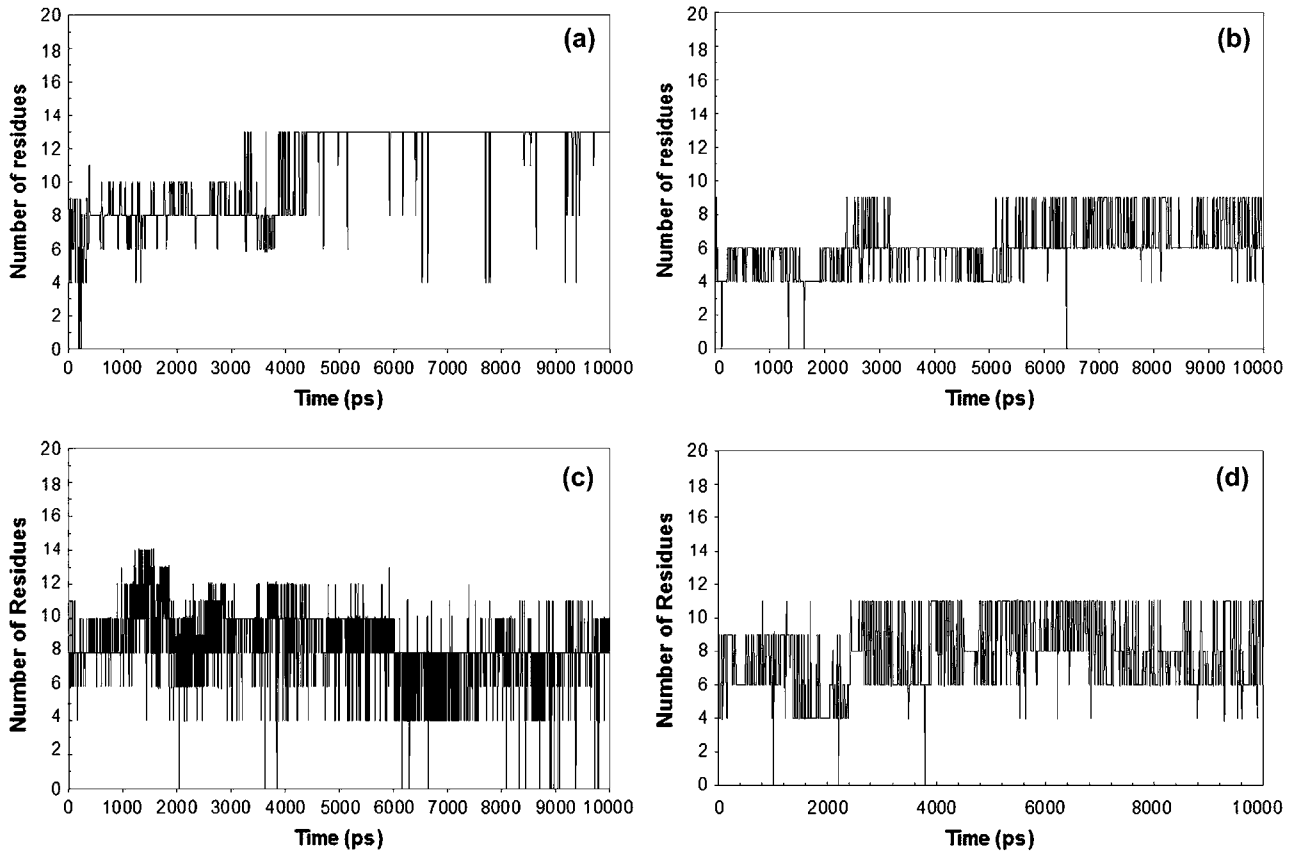

FIGURE 9 Number of residues forming β-sheets as a function of simulation time determined with DSSP during the simulation: (*a*) PVV, (*b*) PPP, (*c*) 1U3M, and (*d*) VVV.

(43,44) and function (45). However, this unique role is attributed to the limited conformation that proline residues confer on the N-C_α rotation and not because of its inability to form β-sheet hydrogen bonding. In addition, this is the first time, to our knowledge, that MD simulations have shown the role of proline in maintaining the secondary structure in such a manner. Nevertheless, further work needs to be done by conducting a survey of existing protein structures to examine if this phenomenon applies to other similarly structured proteins.

REFERENCES

1. Prusiner, S. B. 1991. Molecular biology of prion diseases. *Science.* 252:1515–1522.
2. Pan, K. M., M. Baldwin, J. Nguyen, M. Gasset, A. Serban, D. Groth, I. Mehlhorn, Z. W. Huang, R. J. Fletterick, F. E. Cohen, and S. B. Prusiner. 1993. Conversion of alpha-helices into beta-sheets features in the formation of the scrapie prion proteins. *Proc. Natl. Acad. Sci. USA.* 90:10962–10966.
3. Gasset, M., M. A. Baldwin, R. J. Fletterick, and S. B. Prusiner. 1993. Perturbation of the secondary structure of the scrapie prion protein under conditions that alter infectivity. *Proc. Natl. Acad. Sci. USA.* 90:1–5.
4. Borchelt, D. R., M. Scott, A. Taraboulos, N. Stahl, and S. B. Prusiner. 1990. Scrapie and cellular prion proteins differ in their kinetics of synthesis and topology in cultured cells. *J. Cell Biol.* 110: 743–752.
5. Caughey, B., K. Neary, R. Buller, D. Ernst, L. L. Perry, B. Chesebro, and R. E. Race. 1990. Normal and scrapie-associated forms of prion protein differ in their sensitivities to phospholipase and proteases in intact neuroblastoma cells. *J. Virol.* 64:1093–1101.
6. Brown, P., and L. Cervenakova. 2005. A prion lexicon (out of control). *Lancet.* 365:122.
7. Prusiner, S. B., N. Stahl, and S. J. Dearmond. 1988. Novel mechanisms of degeneration of the central nervous system—prion structure and biology. *Ciba Found. Symp.* 135:239–260.
8. Downing, D. T., and N. D. Lazo. 1999. Molecular modelling indicates that the pathological conformations of prion proteins might be beta-helical. *Biochem. J.* 343:453–460.
9. Carrell, R. W., and D. A. Lomas. 1997. Conformational disease. *Lancet.* 350:134–138.
10. Kopito, R. R., and D. Ron. 2000. Conformational diseases. *Nat. Cell Biol.* 2:208–209.
11. Clarke, A. R., G. S. Jackson, and J. Collinge. 2001. The molecular biology of prion propagation. *Philos. Trans. R. Soc. Lond. B Biol. Sci.* 356:185–194.
12. Li, S. C., N. K. Goto, K. A. Williams, and C. M. Deber. 1996. Alpha-helical, but not beta-sheet, propensity of proline is determined by peptide environment. *Proc. Natl. Acad. Sci. USA.* 93:6676–6681.
13. Reiersen, H., and A. R. Rees. 2001. The hunchback and its neighbours: proline as an environmental modulator. *Trends Biochem. Sci.* 26:679–684.
14. Shamsir, M. S., and A. R. Dalby. 2005. One gene, two diseases and three conformations: molecular dynamics simulations of mutants of

human prion protein at room temperature and elevated temperatures. *Proteins.* 59:275–290.

15. DeMarco, M. L., and V. Daggett. 2004. From conversion to aggregation: protofibril formation of the prion protein. *Proc. Natl. Acad. Sci. USA.* 101:2293–2298.
16. Barducci, A., R. Chelli, P. Procacci, and V. Schettino. 2004. Misfolding pathways of the prion protein probed by molecular dynamics simulations. *Biophys. J.* 88:1334–1343.
17. Alonso, D. O. V., S. J. DeArmond, F. E. Cohen, and V. Daggett. 2001. Mapping the early steps in the pH-induced conformational conversion of the prion protein. *Proc. Natl. Acad. Sci. USA.* 98:2985–2989.
18. Sekijima, M., C. Motono, S. Yamasaki, K. Kaneko, and Y. Akiyama. 2003. Molecular dynamics simulation of dimeric and monomeric forms of human prion protein: insight into dynamics and properties. *Biophys. J.* 85:1176–1185.
19. Gu, W., T. T. Wang, J. Zhu, Y. Y. Shi, and H. Y. Liu. 2003. Molecular dynamics simulation of the unfolding of the human prion protein domain under low pH and high temperature conditions. *Biophys. Chem.* 104:79–94.
20. Kini, R. M., and H. J. Evans. 1995. A hypothetical structural role for proline residues in the flanking segments of protein-protein interaction sites. *Biochem. Biophys. Res. Commun.* 212:1115–1124.
21. Kini, R. M., R. A. Caldwell, Q. Y. Wu, C. M. Baumgarten, J. J. Feher, and H. J. Evans. 1998. Flanking proline residues identify the L-type Ca2+ channel binding site of calciseptine and FS2. *Biochemistry.* 37:9058–9063.
22. Richardson, J. S., and D. C. Richardson. 2002. Natural beta-sheet proteins use negative design to avoid edge-to-edge aggregation. *Proc. Natl. Acad. Sci. USA.* 99:2754–2759.
23. Zahn, R., A. Liu, T. Luhrs, R. Riek, C. von Schroetter, F. Lopez Garcia, M. Billeter, L. Calzolai, G. Wider, and K. Wuthrich. 2000. NMR solution structure of the human prion protein. *Proc. Natl. Acad. Sci. USA.* 97:145–150.
24. Guex, N., and M. C. Peitsch. 1997. SWISS-MODEL and the Swiss-PdbViewer: an environment for comparative protein modeling. *Electrophoresis.* 18:2714–2723.
25. Turk, E., D. B. Teplow, L. E. Hood, and S. B. Prusiner. 1988. Purification and properties of the cellular and scrapie hamster prion proteins. *Eur. J. Biochem.* 176:21–30.
26. Herrmann, L. M., and B. Caughey. 1998. The importance of the disulfide bond in prion protein conversion. *Neuroreport.* 9:2457–2461.
27. Darden, T., D. York, and L. Pedersen. 1993. Particle mesh Ewald: an N·log(N) method for Ewald sums in large systems. *J. Chem. Phys.* 98:10089–10092.
28. Lindahl, E., B. Hess, and D. van der Spoel. 2001. GROMACS 3.0: a package for molecular simulation and trajectory analysis. *J. Mol. Model. (Online).* 7:306–317.
29. Kabsch, W., and C. Sander. 1983. Dictionary of protein secondary structure: pattern recognition of hydrogen-bonded and geometrical features. *Biopolymers.* 22:2577–2637.
30. Delano, W. L. 2002. The PyMOL Molecular Graphics System, DeLano Scientific, San Carlos, CA.
31. Martz, E. 2002. Protein Explorer: easy yet powerful macromolecular visualization. *Trends Biochem. Sci.* 27:107–109.
32. Guilbert, C., F. Ricard, and J. C. Smith. 2000. Dynamic simulation of the mouse prion protein. *Biopolymers.* 54:406–415.
33. Parchment, O. G., and J. W. Essex. 2000. Molecular dynamics of mouse and Syrian hamster PrP: implications for activity. *Proteins.* 38:327–340.
34. Munoz, V., P. A. Thompson, J. Hofrichter, and W. A. Eaton. 1997. Folding dynamics and mechanism of beta-hairpin formation. *Nature.* 390:196–199.
35. De Simone, A., G. G. Dodson, C. S. Verma, A. Zagari, and F. Fraternali. 2005. Prion and water: tight and dynamical hydration sites have a key role in structural stability. *Proc. Natl. Acad. Sci. USA.* 102:7535–7540.
36. Langella, E., R. Improta, and V. Barone. 2004. Checking the pH-induced conformational transition of prion protein by molecular dynamics simulations: effect of protonation of histidine residues. *Biophys. J.* 87:3623–3632.
37. Gsponer, J., P. Ferrara, and A. Caflisch. 2001. Flexibility of the murine prion protein and its Asp178Asn mutant investigated by molecular dynamics simulations. *J. Mol. Graph. Model.* 20:169–182.
38. Calzolai, L., D. A. Lysek, D. R. Perez, P. Guntert, and K. Wuthrich. 2005. Prion protein NMR structures of chickens, turtles, and frogs. *Proc. Natl. Acad. Sci. USA.* 102:651–655.
39. Stanger, H. E., F. A. Syud, J. F. Espinosa, I. Giriat, T. Muir, and S. H. Gellman. 2001. Length-dependent stability and strand length limits in antiparallel beta-sheet secondary structure. *Proc. Natl. Acad. Sci. USA.* 98:12015–12020.
40. Govaerts, C., H. Wille, S. B. Prusiner, and F. E. Cohen. 2004. Evidence for assembly of prions with left-handed β-helices into trimers. *Proc. Natl. Acad. Sci. USA.* 101:8342–8347.
41. Wille, H., M. D. Michelitsch, V. Guenebaut, S. Supattapone, D. J. Segel, D. Walther, H. Serban, S. Doniach, F. E. Cohen, D. A. Agard, and S. B. Prusiner. 2002. Structural studies of the scrapie prion protein by electron crystallography. *Proc. Natl. Acad. Sci. USA.* 99:3563–3568.
42. Wopfner, F., G. Weidenhofer, R. Schneider, A. von Brunn, S. Gilch, T. F. Schwarz, T. Werner, and M. Schatzl. 1999. Analysis of 27 mammalian and 9 avian PrPs reveals high conservation of flexible regions of the prion protein. *J. Mol. Biol.* 289:1163–1178.
43. Zscherp, C., H. Aygun, J. W. Engels, and W. Mantele. 2003. Effect of proline to alanine mutation on the thermal stability of the all-β-sheet protein tendamistat. *Biochim. Biophys. Acta.* 1651:139–145.
44. Nathaniel, C., L. A. Wallace, J. Burke, and H. W. Dirr. 2003. The role of an evolutionarily conserved *cis*-proline in the thioredoxin-like domain of human class Alpha glutathione transferase A1-1. *Biochem. J.* 372:241–246.
45. Cordes, F. S., J. N. Bright, and M. S. P. Sansom. 2002. Proline-induced distortions of transmembrane helices. *J. Mol. Biol.* 323:951–960.